PHYSICAL REVIEW A VOLUME 26, NUMBER 6 DECEMBER 1982

Convection patterns in Fourier space

J. P. Gollub and A. R. McCarriar
Physics Department, Haverford College, Haverford, Pennsylvania 19041
and Physics Department, University of Pennsylvania, Philadelphia, Pennsylvania 19104
(Received 1 July 1982)

Two-dimensional Fourier transforms of convection patterns are computed from data obtained by Doppler scanning of the velocity field. This new technique is used to study the time dependence of the wave-number distribution, and the variation of the mean wave number k^* with Rayleigh number R. We find that k^* increases by about 15% during the pattern evolution following a step change in R from below R_c to $2R_c$. This increase is associated with a reduction in the number of defects in the pattern. The dependence of k^* on R is characterized by a decline above R_c and a steeper decline near $5R_c$ where the skewed varicose instability causes the flow to become time dependent. The peak in the wave-number distribution does not shift significantly in the range $6-40R_c$, and still contains about half of the spectral power at $40R_c$. The flow apparently remains largely two dimensional.

I. INTRODUCTION

Above the critical Rayleigh number R_c, a laterally infinite fluid layer between thermally conducting boundaries can achieve a steady flow consisting of parallel rolls, according to nonlinear stability theory.[1] However, the existence of orientational degeneracy and a band of stable roll wave numbers indicates that processes of pattern selection, which are not contained in the usual stability theory, must occur. Some theoretical progress in treating pattern selection has been made recently.[2-5]

Earlier experiments in a large rectangular cell showed that there are multiple stable patterns at a given R.[6,7] Furthermore, a state in which the rolls are parallel everywhere in the cell is never reached. Instead, they align approximately perpendicular to all lateral boundaries in a large layer. This causes curvature and defects in the patterns. A change in R induces patterns with many defects which evolve toward simpler patterns over periods much longer than the natural hydrodynamic time scale for the Rayleigh-Benard instability, the vertical thermal diffusion time τ_v across the fluid layer. In some cases, the patterns remain slowly time dependent for at least $10\,000\tau_v$. This failure to reach a steady flow may be related to earlier observations by Ahlers and Walden[8] in which the effective thermal conductivity of a layer of convecting liquid helium was found to be noisy not far above R_c.

In the present paper, we report experiments in which spatial Fourier analysis was performed on data obtained by Doppler scanning of the velocity field. Two-dimensional Fourier transforms have not been previously used in experimental studies of thermal convection or other instabilities. This powerful technique allows quantitative study, for example, of the wave-number distributions of convective flows as a function of both time and Rayleigh number. It permits us to address questions such as these: Does pattern evolution involve changes in the mean wave number, changes in the angular distribution in wave-number space, or both? What changes in the wave-number distribution are associated with particular instabilities? How does the wave-number distribution depend on the Rayleigh number or on the nature of the pattern?

In Sec. II we explain how two-dimensional Fourier spectra were obtained, followed by presentation of results on pattern evolution and the dependence of the wave-number distribution on Rayleigh number in Secs. III and IV. The relation of our work to theoretical studies and other experiments is discussed in Sec. V.

II. OBTAINING FOURIER SPECTRA OF PATTERNS

The apparatus and laser Doppler mapping technique have been described elsewhere,[7] and will be only briefly summarized. The interior horizontal dimensions of the cell are approximately 15×10 cm^2, the layer depth is $d=0.5$ cm, and the fluid is confined between copper plates whose temperatures are controlled electronically. The Rayleigh number

is stable to better than 1% over periods of several weeks. The working fluid is water at about 70°C where the Prandtl number (the ratio of the kinematic viscosity to the thermal diffusivity of the fluid) is 2.5. The time τ_v required for heat to diffuse vertically across the fluid layer is 170 s, and the time for heat to diffuse horizontally the full length of the cell is 40 h. These are the natural hydrodynamic time scales.

Laser Doppler velocimetry is used to map the local velocity component parallel to the long cell edge by translation in two dimensions under computer control. The velocity field can be mapped in a horizontal plane in about an hour (several thousand measurements). Below $5R_c$, where the time dependence is exceedingly slow, the result is an effectively instantaneous digital record of the flow field in a plane.

One way to display the results of such a Doppler scan is to plot contour maps of constant Doppler shift (constant velocity parallel to the long cell edge). An example is shown in Fig. 1(a), obtained at $4.03R_c$. The diagram represents the flow in a plane located a distance $d/4$ below the top of the cell. Each dot is a location at which the velocity component parallel to the long cell edge is found to be zero. The loci of these dots define the boundaries of the convective rolls. The actual flow direction at the location of the dots is out of or into the page, alternating from one row of dots to the next. Equivalently, the vorticity is opposite in adjacent rolls. As noted earlier,[6,7] the rolls align perpendicular to the four lateral cell boundaries, causing roll curvature and a pair of localized defects in the pattern. This particular pattern is only one of several that can be obtained at the same Rayleigh number.

The next step in the analysis is to construct the two-dimensional power spectrum (the magnitude squared of the Fourier transform) of the 2646 points in the data array of velocity measurements. This is easily achieved in a few minutes on an LSI 11/23 computer with a one-dimensional fast Fourier transform algorithm by first transforming each row and then each column of the data array, after application of a cosine taper. The power spectrum (magnitude squared of the Fourier transform) corresponding to the velocity map of Fig. 1(a) is displayed as a function of the x and y components of the wave number in Fig. 1(b). (All wave numbers in this paper have been divided by 2π, so that the critical wave number k_c in these units is 0.95

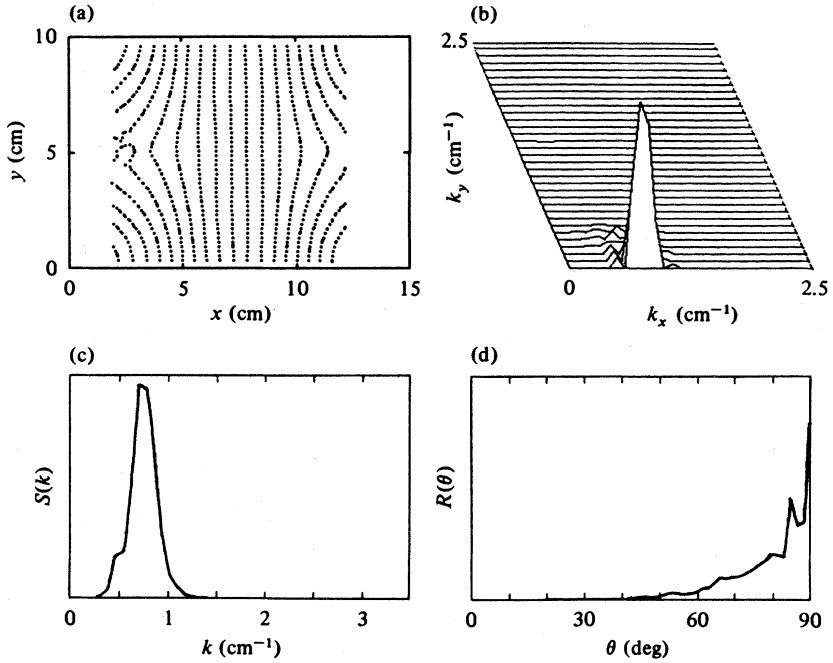

FIG. 1. (a) Doppler map of the velocity field for a stable symmetric convective flow at $4.03R_c$. The dots are locations at which the flow is entirely vertical, i.e., the roll boundaries. (b) Two-dimensional Fourier spectrum $P(k_x,k_y)$ of the 2946-point data array from which the map was made, on a linear scale. (c) Wave-number distribution $S(k)$ formed by integrating the Fourier spectrum along circular arcs. (d) Angular distribution $Q(\theta)$ formed by integrating the Fourier spectrum along radial lines in wave-number space.

cm^{-1}.) In this case, there is clearly a peak on the k_x axis due to the alignment of rolls parallel to the y axis in real space.

We have found it useful to change to circular coordinates (k,θ) in $\vec{k}$ space and to construct two auxiliary functions by integrating along radial lines and circular arcs. If $P(k_x,k_y)$ is the power spectrum, we integrate along a circular arc at fixed radius k to obtain the function $S(k)$ defined by

$$S(k)=\int P(k\sin(\theta),k\cos(\theta))k\,dk\ .$$

Since the spectrum is only known at discrete points in wave-number space, it is necessary to interpolate in order to compute this integral. Note that k can be larger than either k_x or k_y, so that its limit is somewhat larger than the Nyquist frequency in either direction (2.5 cm^{-1} in this case). The resulting function $S(k)$, which we call the wave-number distribution, is plotted in Fig. 1(c). It has a well-defined peak whose first moment is at 0.75 cm^{-1}, and whose linewidth (square root of the second moment) is 0.14 cm^{-1}. This width is somewhat greater than the instrumental resolution determined by the inverse cell size, 0.10 cm^{-1}, and is a reflection of the fact that the roll spacing varies because of the defects or nonuniform spacing in the pattern.

The second auxiliary function $Q(\theta)$ is obtained by integrating over radial lines in $\vec{k}$ space:

$$Q(\theta)=\int P(k\sin(\theta),k\cos(\theta))k\,d(\theta)\ .$$

The result, shown in Fig. 1(d), has a peak at $\theta=90$ deg (measured from the k_y axis) as expected. Its width reflects the curvature in the roll pattern.

Above $5R_c$, the Doppler maps are not instantaneous, since the flow changes significantly during the mapping process. However, we find that the main features of the flow are still correctly obtained, because the mapping is made in lines parallel to the long cell axis; each line is acquired in about one minute. In order to test for distortion in $S(k)$ due to the motion, we also performed one-dimensional line scans parallel to (and near) the long cell edge, where the rolls tend to be locally perpendicular to the direction of the scan. The resulting spectral density and wave-number distribution were quite close to those obtained from two-dimensional scans over the entire cell. We also found that wave-number distributions computed from maps of different size, requiring different time intervals, were essentially the same. Thus, we believe that the two-dimensional spectral density is semiquantitatively correct even in the time-dependent regimes. Obviously, it would be better to use a technique that maps the velocity field more quickly. The limitation on mapping speed is mainly in the time (about 1 s) required to accumulate a Doppler measurement with adequate signal-to-noise ratio, not in the time to move from one location to the next.

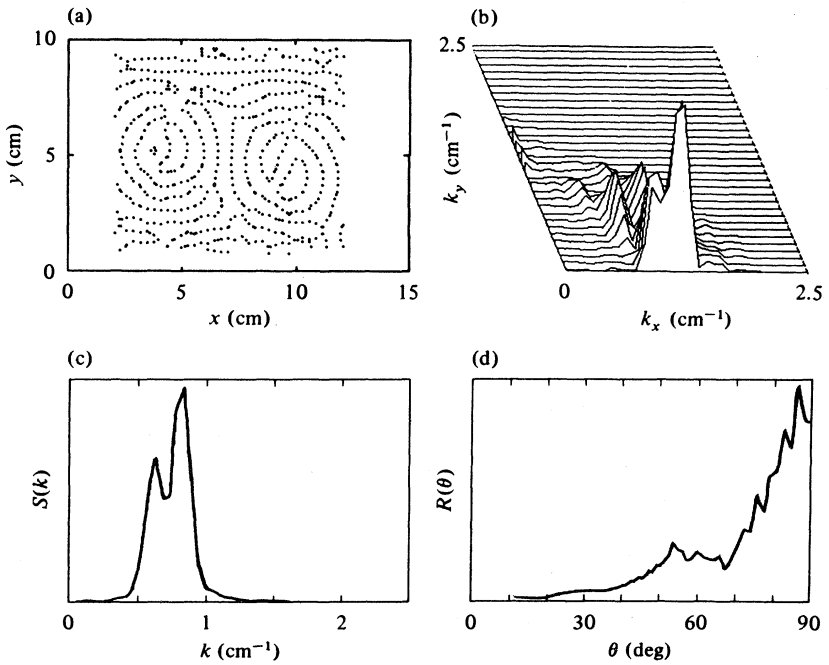

FIG. 2. (a)—(d) Doppler map, spectrum, wave-number distribution $S(k)$, and angular distribution $Q(\theta)$ soon after the Rayleigh number was increased to $2.0R_c$. See caption for Fig. 1.

III. PATTERN EVOLUTION

We studied the evolution of patterns by the following procedure. The Rayleigh number was left at $0.4R_c$ overnight and then suddenly increased to $2.0R_c$. The flow was then mapped hourly over at least 24 hours, and sometimes several hundred hours, about 5 horizontal thermal diffusion times. Many separate runs were made in this way.

The flow pattern an hour after the change in R is typically complex with many defects, as shown in Fig. 2(a). At this early stage, the rolls are not yet perpendicular to the boundaries. The wave-number distribution $S(k)$, Fig. 2(c), has a well-defined peak that is not significantly broader than the one in Fig. 1(c). However, the angular distribution $Q(\theta)$, Fig. 2(d), is more spread out than the corresponding example in Fig. 1(d) because of the disorder in the pattern.

We followed the process of pattern evolution by mapping the flow approximately once per hour. The evolution is a noisy process, in which the local velocity changes erratically over a period of a day or two (roughly one horizontal thermal diffusion time), as defects are expelled and the pattern becomes more orderly. (In some runs, slow time dependence persists for at least a few hundred hours, and perhaps indefinitely. However, the character of this time dependence is different after the first day or two. The simplification of the pattern occurs during this earlier period.)

For comparison, we show in Fig. 3 the map and spectrum 256 hours after the start of the run. There are fewer defects and the rate of change is quite slow, but a symmetric flow has not been reached. The evolution in Fourier space is not dramatic. Comparing Figs. 2 and 3, we find that the first moment of the peak has increased from 0.75 to 0.86 cm^{-1} while the linewidth has changed slightly (0.14 to 0.156 cm^{-1}). The angular distribution $Q(\theta)$ has narrowed in this case, from 0.29 to 0.21 cm^{-1}. However, in other runs we do not find a monotonic decrease in the width of $Q(\theta)$, because the boundaries cause orientations with positive k_y in some parts of the cell.

The major consistent feature of the pattern evolution in wave-number space is the increase in the first moment k^* of the peak as the number of defects in the pattern decreases. That is, the wave-number distribution shifts slightly to higher k. This effect is shown more clearly in Fig. 4, where the first moment is plotted as a function of time for several different runs made at $2.0R_c$. The rise of 10—15% is not large, but is statistically significant. Apparently, the excessive number of defects found at early times forces the patterns to be less

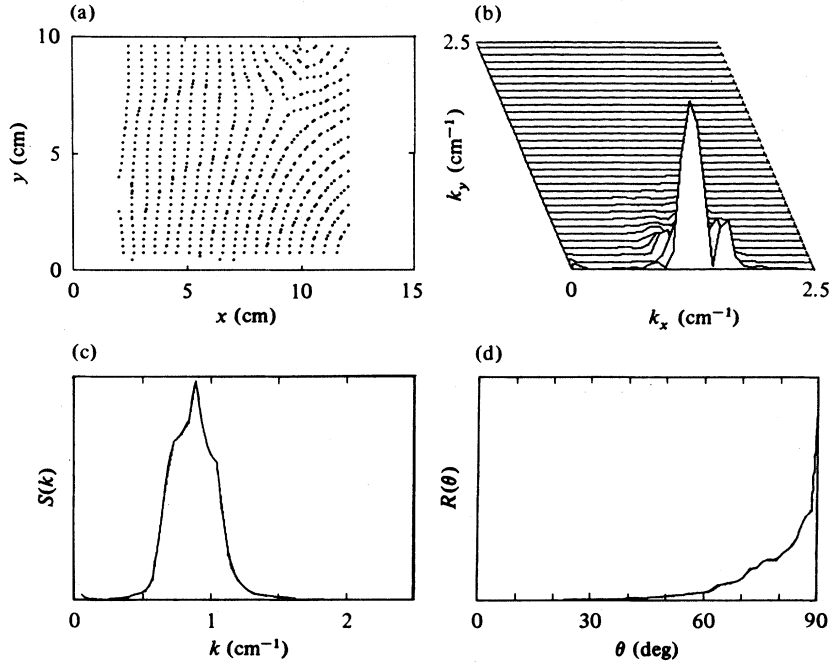

FIG. 3. (a)—(d) Doppler map, spectrum, wave-number distribution $S(k)$, and angular distribution $Q(\theta)$ 256 hours after the Rayleigh number was increased to $2.0R_c$. The flow is now evolving quite slowly and the mean wave number has increased somewhat. See caption for Fig. 1.

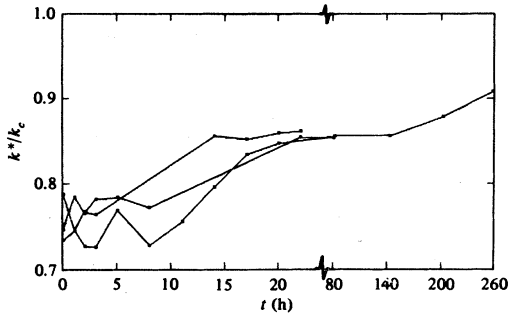

FIG. 4. Time evolution of the mean wave number k^* of the peak in $S(k)$ after the Rayleigh number was increased to $2.0R_c$ in several separate runs. Note the change in the time scale used to show the latter part of the longest run.

compact than they are later. (However, even in the long-time limit, the mean wave number is below the critical value for Rayleigh numbers above R_c, as we discuss more extensively in Sec. IV.) We also find that pattern evolution following a *decrease* from $40R_c$ to $2R_c$ shows a monotonically rising mean wave number, but starting from a lower initial value.

IV. RAYLEIGH NUMBER DEPENDENCE OF THE WAVE-NUMBER DISTRIBUTION

In this section, we describe measurements of the wave-number distribution after the transient pattern evolution, as a function of Rayleigh number. Above $5R_c$ the patterns are always time dependent, as we noted earlier.[6,7] The onset of this faster (and noisy) time dependence has been linked to the "skewed varicose instability" of Busse and Clever.[9] An example of a map made at $33R_c$ is shown in Fig. 5(a). A clearly defined characteristic scale is visible, with a predominant wave vector along k_x. This scale is also manifested by a region of high spectral density on the k_x axis of Fig. 5(b) and by the peak in the wave-number distribution $S(k)$, Fig. 5(c). There is significant noise at high wave number, but the peak at wave numbers comparable to the inverse layer thickness dominates even at $40R_c$.

The angular distribution $Q(\theta)$ in the time-dependent regime is typically quite broad, as shown in Fig. 5(d). However, this function is likely to be distorted by the motion, and cannot be interpreted quantitatively.

The first moment k^* of the peak in the wave-number distribution $S(k)$ is shown as a function of $\epsilon=(R-R_c)/R_c$ in Fig. 6. We find that the variability in this quantity from one pattern to the next is about $\pm 5\%$ from the mean in either direction, provided sufficient time is allowed before making measurements, and we do not find clear evidence of hysteresis in the ordinary sense. We typically average over several patterns at each Rayleigh number to reduce the variability. The wave numbers have been normalized by the predicted critical wave

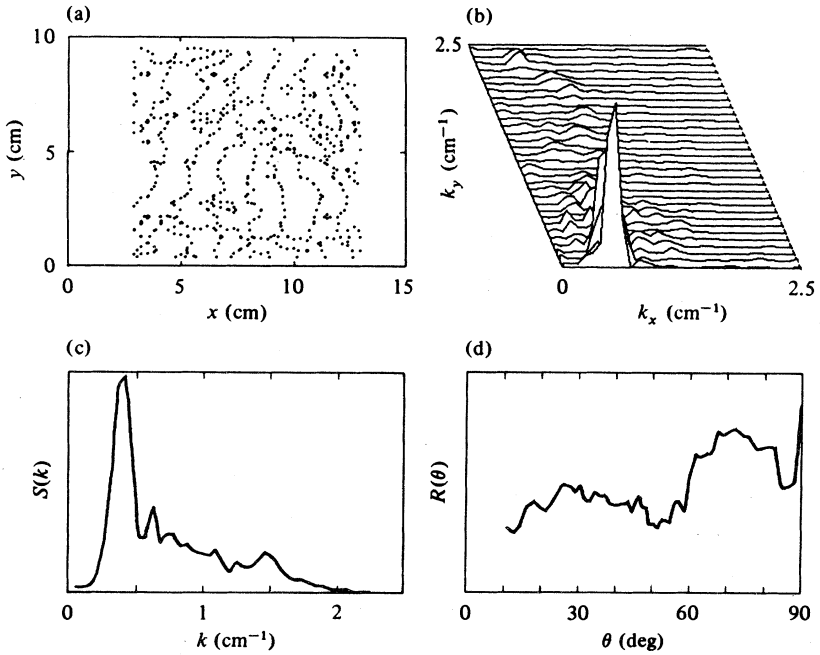

FIG. 5. (a)—(d) Doppler map, spectrum, wave-number distribution $S(k)$, and angular distribution $Q(\theta)$ at high Rayleigh number ($33R_c$), where the flow is strongly time dependent. See caption for Fig. 1.

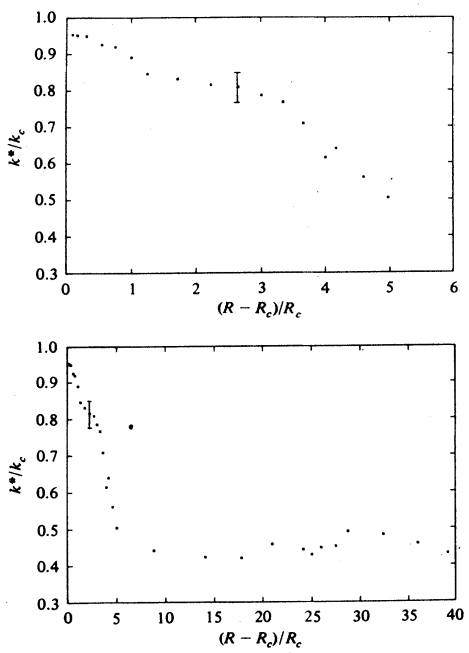

FIG. 6. Mean wave number k^* of the peak in $S(k)$ normalized by the critical wave number k_c, as a function of Rayleigh number, on two different scales. There is a steep decline at the onset of rapid time dependence, but little further change at high R.

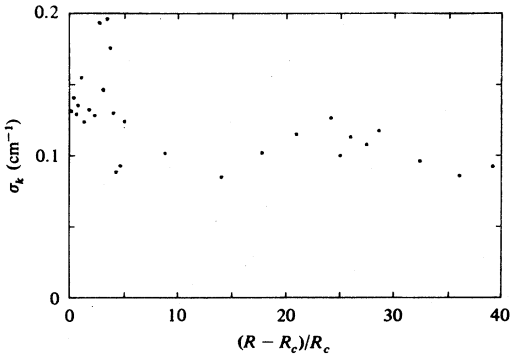

FIG. 7. Linewidth of the spectral peak in $S(k)$ as a function of Rayleigh number. For comparison, note that k_c is 0.95 cm^{-1}, so that the width is typically 10–20% of k_c.

number k_c for the onset of convection. In computing the first moment, a cutoff is applied to exclude the high wave-number noise at high R. The curve has a number of interesting properties:

(a) As R approaches R_c, k seems to approach $0.95k_c$, about 5% lower than the predicted value. This reduction is probably due to defects in the pattern, which are still noticeable at low R.

(b) The mean wave number declines monotonically as R increases. We are unable to say whether the apparent leveling off near $\epsilon=1$ is real or is rather due to inadequate averaging over different patterns.

(c) The rate of decline increases in the range $3<\epsilon<5$, near the onset of the skewed varicose instability, where rapid time dependence begins. This decline in the mean wave number is related to the pinching off of rolls which we detected earlier[6,7] by repetitive mapping at $5R_c$.

(d) The mean wave number of the peak is approximately constant from $\epsilon=6$ to $\epsilon=40$. There is no detectable change at the onset of the oscillatory instability, which occurs[7,9] at about $\epsilon=8$ at the Prandtl number used in these experiments. However, at $\epsilon=40$, the spectral power at wave numbers above the peak is about half of the total power. (This power has been excluded in computing the mean wave number of the peak. The mean wave number of the entire spectrum does increase at high R.) We have also computed the linewidth of the peak in $S(k)$ (square root of the second moment). This quantity is shown as a function of ϵ in Fig. 7. Though there are significant fluctuations from run to run, the linewidth does not increase with R, and it even decreases somewhat as the peak shifts to lower wave number. Typical linewidths are 10–20% of k_c.

V. DISCUSSION AND CONCLUSIONS

We find that the most significant change in Fourier space during pattern evolution is a small increase (about 15%) in the mean wave number k^* as the defects are eliminated. This change occurs in about one day, a time comparable to the horizontal thermal diffusion time. The pattern evolution typically continues after that, but at a reduced rate and with out further reproducible change in the wave-number distribution $S(k)$ or in the angular distribution $Q(\theta)$. The small magnitude of the observed increase in k^* may be related to the long-time scale of the evolution. If k^* were to shift dramatically, the process would presumably occur more quickly.

The mean wave number declines with Rayleigh number, with much of the decline apparently associated with the approach to the skewed varicose instability, a long-wavelength deformation that causes the flow to be time dependent above $5R_c$. According to the calculations of Busse and Clever,[9] the wave number of stable rolls must lie in a "balloon" bounded by the neutral stability curve (R vs k) and the stability boundaries of various secondary instabilities, especially the skewed varicose (SV) instabili-

ty. The fact that the SV onset shifts to lower k as R increases may account for the basic decline in k^* with R.[10]

The width of the wave-number distribution does not increase with R. In the range above $2R_c$, both the width of $S(k)$ (about $0.15k^*$) and the variability of k^* from one pattern to another ($\pm 5\%$) are clearly less than is permitted by the linear stability theory for the infinite layer. Therefore, some form of pattern selection is occurring. However, we are unable to separate the roles of the boundaries and the secondary instabilities in controlling this process.

At high R, we find that much of the power in the spatial spectrum is still in the peak located at about $0.5k_c$, and the position of the peak does not shift significantly between $6R_c$ and $40R_c$. These observations suggest that the motion is largely two dimensional even at $40R_c$, though time records made at any location in the flow are extremely noisy.

Willis, Deardorff, and Somerville[11] have reported measurements of the mean roll wavelength for air (Prandtl number 0.67) by manual analysis of photographs. Their results show a decline in the mean wave number above R_c (as Koshmieder[12] has noted at much higher Prandtl number), but there is no evidence of the more rapid decline we find near the onset of the skewed varicose instability. They also found that the slope of the mean wave number moderates at high R. These measurements did not extend over periods comparable to the horizontal thermal diffusion time.

Cross[2] has recently discussed a model based on a Lyapunov functional F whose minimization governs the relative stability of various possible patterns in the regime asymptotically near R_c. He showed that there are three competing contributions to F: a term associated with roll orientation at the lateral boundaries, a term associated with roll curvature in the bulk, and a term due to defects. The competition between these contributions is clearly visible in the patterns we observe and may govern the evolution process. However, a potential theory of this type is expected to apply quantitatively only near R_c.[3]

Greenside[4] has recently done a numerical study of the amplitude equation which can be derived from this model. It gives the evolution in time and two space dimensions of the local roll amplitude. Computations were done for cell dimensions similar to those of the present experiments. Greenside finds that pattern evolution requiring many horizontal thermal diffusion times occurs at $\epsilon = 0.1$, beginning with random initial conditions. However, the evolution in the wave-number distribution is minimal, and the mean wave number is always close to k_c. Unfortunately, a direct comparison with the experiments is not yet possible because the model is best where the experiments are difficult, very near R_c. Improvements in both the model and the experiments may make a quantitative comparison more meaningful in the future.

In conclusion, we note that spatial Fourier analysis permits quantitative studies of pattern evolution resulting from hydrodynamic instabilities, and might be effectively used in other nonlinear problems involving time-dependent fields, provided suitable instrumentation can be devised.

ACKNOWLEDGMENTS

We appreciate numerous helpful discussions with H. Greenside and thank him for sharing the results of his numerical computations with us prior to publication. This work was supported by National Science Foundation Grant No. MEA-7912150.

[1]F. H. Busse, Rep. Prog. Phys. 41, 1929 (1978).
[2]M. C. Cross, Phys. Rev. A 25, 1065 (1982).
[3]E. D. Siggia and A. Zippelius, Phys. Rev. Lett. 47, 835 (1981).
[4]H. Greenside, W. M. Coughran, Jr., and N. L. Schryer, Phys. Rev. Lett. 49, 726 (1982).
[5]L. Kramer, E. Ben-Jacob, and H. Brand (unpublished).
[6]J. P. Gollub and J. F. Steinman, Phys. Rev. Lett. 47, 505 (1981).
[7]J. P. Gollub, A. R. McCarrier, and J. F. Steinman, J. Fluid Mech. (in press).
[8]G. Ahers and R. W. Walden, Phys. Rev. Lett. 44, 445 (1980).
[9]F. H. Busse and R. M. Clever, J. Fluid Mech. 91, 319 (1979).
[10]R. M. Clever and F. H. Busse, J. Appl. Math. Phys. (ZAMP) 29, 711 (1978).
[11]G. E. Willis, J. W. Deardorff, and R. C. J. Somerville, J. Fluid Mech. 54, 351 (1972).
[12]E. L. Koschmieder, in *Advances in Chemical Physics*, Vol. 26, edited by I. Prigogine and S. A. Rice (Wiley, New York, 1974), p. 177.